X-Ray Data Booklet

Section 4.1 MULTILAYERS AND CRYSTALS

James H. Underwood

A. MULTILAYERS

By means of modern vacuum deposition technology, structures consisting of alternating layers of high- and low-Z materials, with individual layers having thicknesses of the order of nanometers, can be fabricated on suitable substrates. These structures act as multilayer interference reflectors for x-rays, soft x-rays, and extreme ultraviolet (EUV) light. Their high reflectivity and moderate energy bandwidth ($10 < E/\Delta E < 100$) make them a valuable addition to the range of optical components useful in instrumentation for EUV radiation and x-rays with photon energies from a few hundred eV to tens of keV. These multilayers are particularly useful as mirrors and dispersive elements on synchrotron radiation beamlines. They may be used to produce focal spots with micrometer-scale sizes and for applications such as fluorescent microprobing, microdiffraction, and microcrystallography. Multilayer reflectors also have a wide range of applications in the EUV region, where normal-incidence multilayer reflectors allow the construction of space telescopes and of optics for EUV lithography.

Ordinary mirrors, operating at normal or near-normal angles of incidence, do not work throughout the EUV and x-ray regions. The reason is the value of the complex refractive index, $n = 1 - \delta - i\beta$, which can be close to unity for all materials in this region; δ may vary between 10^{-3} in the EUV region to 10^{-6} in the x-ray region. The Fresnel equations at normal incidence show that the reflectivity $R^2 = |(n-1)/(n+1)|^2$ is very small. However, the more general Fresnel equations show that x-rays and EUV radiation can be reflected by mirrors at large angles of incidence. Glancing (or grazing) incidence is the term used when the rays make a small angle (a few degrees or less) with the mirror surface; the complement ($90° - i$) of the optical angle of incidence i is called the glancing (or grazing) angle of incidence. Glancing-incidence mirrors are discussed in Section 4.2.

Although the normal-incidence intensity reflectivity R^2 of a surface might be 10^{-3} or 10^{-4}, the corresponding *amplitude* reflectivity $R = (n-1)/(n+1)$, the square root of the intensity reflectivity, will be 1/30 to 1/100. This implies that, if the reflections from 30–100 surfaces could be made to add in phase, a total reflectivity approaching unity could be obtained. This is the multilayer principle. As shown in Fig. 4-1, a multilayer reflector comprises a stack of materials having alternately high and low refractive indices. The thicknesses are adjusted so that the path length difference between reflections from successive layer pairs is equal to one wavelength. Hence, x-ray/EUV multilayers are approximately equivalent to the familiar "quarter-wave stacks" of visible-light coating technology. The equivalence is not exact, however, because of the absorption term β, which is usually negligible for visible-light multilayers. This absorption reduces the multilayer reflectivity below unity and requires the design to be optimized for highest reflectivity. Particularly critical is the value of Γ, which is the ratio of the thickness of the high-Z (high electron density, high $|n|$) layer to the total thickness of each layer pair. This optimization

normally requires modeling or simulation of the multilayer. Most thin-film calculation programs, even if designed for the visible region, will perform these calculations if given the right complex values of the refractive index. Alternatively, there are a number of on-line calculation programs available; links can be found at http://www-cxro.lbl.gov/.

Either elemental materials or compounds can be used to fabricate multilayer reflectors. The performance obtained from a multilayer depends largely on whether there exists a fortuituous combination of materials having the right refractive indices (good contrast, low absorption), whether these materials can be deposited in smooth thin layers, and whether they remain stable (low reactivity, low diffusion) in the deposited state. The roughness of the underlying substrate is also of prime importance; an rms roughness of the same order of magnitude as the layer

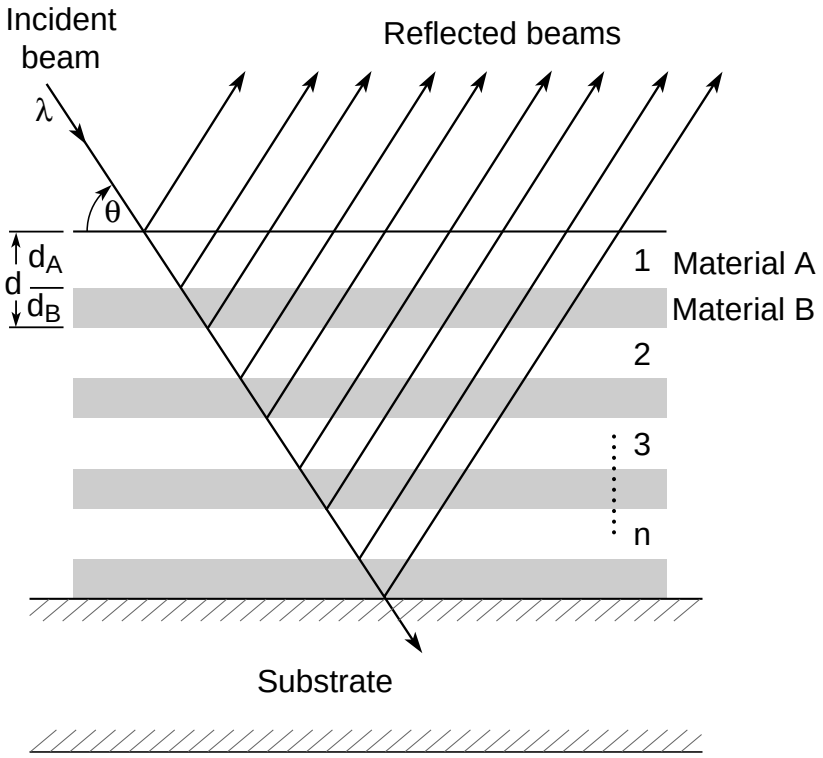

Fig. 4-1. *Schematic of a multilayer reflector of n bilayer pairs. The parameters λ, θ, and d are chosen to satisfy the familiar Bragg equation, but the relative thicknesses of the high- and low-Z materials are also critical in optimizing reflectivity. The total reflectivity is the vector sum of the complex reflection coefficients at each interface, with the different path lengths taken into account.*

thicknesses will spoil the performance of most coatings. "Superpolished" substrates, with roughness $\sigma \approx 0.1$ nm are preferred. On such substrates, the peak reflectivity of the coatings can approach 80% to 90% of theoretical predictions.

A large variety of multilayers have been made and their reflectivities measured over the years. A database of reported reflectivities has been assembled from surveys taken at the biennial Physics of X-ray Multilayer Structures conferences and can be found at the website listed above. For the EUV region around 100 eV, two remarkably successful combinations are molybdenum-silicon and molybdenum-beryllium. With Mo-Si, a normal-incidence reflectivity of 68% has been achieved at a wavelength of 13.4 nm; Mo-Be multilayers have achieved a reflectivity close

to 70% at 11.4 nm (see Fig. 4-2). These relatively high reflectivities are the basis for current efforts in the field of EUV lithography.

At hard x-ray wavelengths near 10 keV, a commonly used multilayer is made with tungsten as the high-Z material and boron carbide (B_4C) as the low-Z material. A reflectivity of 84% has been achieved with this combination at 8048 eV, the energy of the Cu $K\alpha$ line (see Fig. 4-3).

B. CRYSTALS

Multilayers are examples of a periodic structure that can be used to analyze short-wavelength electromagnetic radiation. Such structures split the incident beam into a large number N of separate beams; between any beam i and the beam $i + 1$, the optical path difference is constant. After leaving the periodic structure, the beams are recombined and caused to interfere, whereupon the spectrum of the incident radiation is produced.

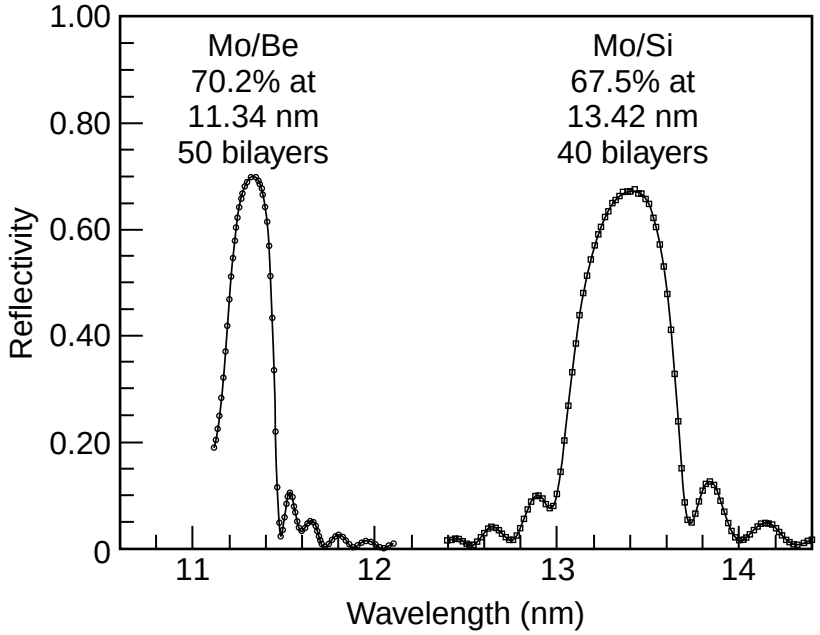

Fig. 4-2. *The reflectivity of two multilayer reflectors at extreme ultraviolet wavelengths.*

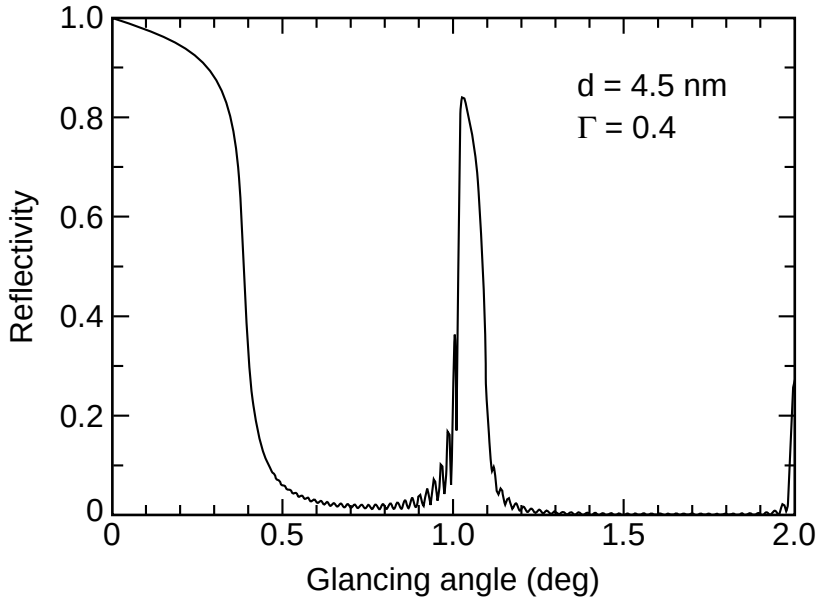

Fig. 4-3. *The reflectivity of a tungsten–boron carbide multilayer at 8048 eV. The parameters d and* Γ *are discussed in the text.*

Dispersion of radiation by a periodic structure is thus formally equivalent to multiple-beam interferometry. Structures that are periodic across their surface and that produce the N interfering beams by division of the incident wave front are called gratings and are treated in Section 4.3. Crystals and multilayer structures produce the N interfering beams by division of the incident *amplitude*. The spectrum of the incident radiation is dispersed in angle according to the Bragg equation $n\lambda = 2d \sin \theta$, where n is an integer representing the order of the reflection, λ is the wavelength of the incident radiation, d is the period of the multilayer or crystal structure, and θ is the angle of glancing incidence. For a crystal, d is the lattice spacing, the perpendicular distance between the successive planes of atoms contributing to the reflection. These planes are designated by their Miller indices [(*hkl*) or, in the case of crystals belonging to the hexagonal group, (*hkil*)]. (The value of $2d$ also represents the longest wavelength that the structure can diffract.)

For $2d$ values greater than about 25 Å, the choice of natural crystals is very limited, and those available (such as prochlorite) are likely to be small and of poor quality. Sputtered or evaporated multilayers can be used as dispersing elements at longer wavelengths. (Langmuir-Blodgett films have fallen into disfavor since the development of vacuum-deposited multilayers.)

Table 4-1 is a revision of one compiled by E. P. Bertin [1]. The crystals are arranged in order of increasing $2d$ spacing.

REFERENCE

1. E. P. Bertin, "Crystals and Multilayer Langmuir-Blodgett Films Used as Analyzers in Wavelength-Dispersive X-Ray Spectrometers," in J. W. Robinson, Ed., *Handbook of Spectroscopy* (CRC Press, Cleveland, 1974), vol. 1, p. 238.

Table 4-1. *Data for selected crystals used as dispersive elements in x-ray spectrometers and monochromators. The Miller indices [(hkl), or (hkil) for hexagonal crystals] are given for the diffracting planes parallel to the surface of the dispersive element. A question mark (?) indicates that the crystal is developmental and that the indices have not been ascertained. An asterisk following the indices indicates that literature references to this crystal without specification of (hkl) or 2d are likely to be references to this "cut." The indicated useful wavelength region lies in the 2θ interval between 10° and 140°. The analyzer should be used outside this region in special cases only.*

No.	Crystal	Miller indices	2*d* (Å)	Chemical formula	Useful wavelength region (Å)	Applications, remarks
1	α-Quartz, silicon dioxide	$(50\bar{5}2)$	1.624	SiO_2	0.142–1.55	Shortest 2*d* of any practical crystal. Good for high-*Z* *K*-lines excited by 100-kV generators.
2	Lithium fluoride	(422)	1.652	LiF	0.144–1.58	Better than quartz $(50\bar{5}2)$ for the same applications.
3	Corundum, aluminum oxide	(146)	1.660	Al_2O_3	0.145–1.58	Same applications as quartz $(50\bar{5}2)$
4	Lithium fluoride	(420)	1.801	LiF	0.157–1.72	Similar to LiF (422).
5	Calcite, calcium carbonate	(633)	2.02	$CaCO_3$	0.176–1.95	
6	α-Quartz, silicon dioxide	$(22\bar{4}3)$	2.024	SiO_2	0.177–1.96	
7	α-Quartz, silicon dixoide	$(31\bar{4}0)$	2.3604	SiO_2	0.205–2.25	Transmission-crystal optics.
8	α-Quartz, silicon dioxide	$(22\bar{4}0)$	2.451	SiO_2	0.213–2.37	
9	Topaz, hydrated aluminum fluorosilicate	(303)*	2.712	$Al_2(F,OH)_2SiO_4$	0.236–2.59	Improves dispersion for V–Ni *K*-lines and rare earth *L*-lines.
10	Corundum, aluminum oxide, sapphire, alumina	(030)	2.748	Al_2O_3	0.240–2.62	Diffracted intensity ~2–4X topaz (303) and quartz (203) with the same or better resolution.
11	α-Quartz, silicon dioxide	$(20\bar{2}3)$	2.749	SiO_2	0.240–2.62	Same applications as topaz (303) and LiF (220).

Table 4-1. *Selected data for crystals (continued).*

No.	Crystal	Miller indices	2*d* (Å)	Chemical formula	Useful wavelength region (Å)	Applications, remarks
12	Topaz	(006)	2.795	$Al_2(F,OH)_2SiO_4$	0.244–2.67	
13	Lithium fluoride	(220)	2.848	LiF	0.248–2.72	Same applications as topaz (303) and quartz $(20\bar{2}3)$, with 2–4X their diffracted intensity. Diffracted intensity ~0.4–0.8X LiF (200).
14	Mica, muscovite	(331)	3.00	$K_2O{\cdot}3Al_2O_3{\cdot}6SiO_2{\cdot}2H_2O$	0.262–2.86	Transmission-crystal optics (Cauchois, DuMond types).
15	Calcite, calcium carbonate	(422)	3.034	$CaCO_3$	0.264–2.93	
16	α-Quartz, silicon dioxide	$(21\bar{3}1)$	3.082	SiO_2	0.269–2.94	
17	α-Quartz, silicon dioxide	$(11\bar{2}2)$	3.636	SiO_2	0.317–3.47	
18	Silicon	(220)	3.8403117	Si	0.335–3.66	Lattice period known to high accuracy.
19	Fluorite, calcium fluoride	(220)	3.862	CaF_2	0.337–3.68	
20	Germanium	(220)	4.00	Ge	0.349–3.82	
21	Lithium fluoride	(200)*	4.027	LiF	0.351–384	Best general crystal for K *K*- to Lr *L*-lines. Highest intensity for largest number of elements of any crystal. Combines high intensity and high dispersion.
22	Aluminum	(200)	4.048	Al	0.353–3.86	Curved, especially doubly curved, optics.
23	α-Quartz, silicon dioxide	$(20\bar{2}0)$	4.246	SiO_2	0.370–4.11	"Prism" cut.
24	α-Quartz, silicon dioxide	$(10\bar{1}2)$	4.564	SiO_2	0.398–4.35	Used in prototype Laue multichannel spectrometer.
25	Topaz	(200)	4.638	$Al_2(F,OH)_2SiO_4$	0.405–4.43	

Table 4-1. *Selected data for crystals (continued).*

No.	Crystal	Miller indices	2*d* (Å)	Chemical formula	Useful wavelength region (Å)	Applications, remarks
26	Aluminum	(111)	4.676	Al	0.408–4.46	Curved, especially doubly curved, optics.
27	α-Quartz, silicon dioxide	$(11\bar{2}0)$	4.912	SiO_2	0.428–4.75	
28	Gypsum, calcium sulfate dihydrate	(002)	4.990	$CaSO_4{\cdot}2H_2O$	0.435–4.76	Efflorescent: loses water in vacuum to become Plaster of Paris.
29	Rock salt, sodium chloride	(200)	5.641	NaCl	0.492–5.38	S $K\alpha$ and Cl $K\alpha$ in light matrixes. Like LiF (200), good general crystal for S *K* to Lr *L*.
30	Calcite, calcium carbonate	(200)	6.071	$CaCO_3$	0.529–5.79	Very precise wavelength measurements. Extremely high degree of crystal perfection with resultant sharp lines.
31	Ammonium dihydrogen phosphate (ADP)	(112)	6.14	$NH_4H_2PO_4$	0.535–5.86	
32	Silicon	(111)*	6.2712	Si	0.547–5.98	Very rugged and stable general-purpose crystal. High degree of perfection obtainable.
33	Sylvite, potassium chloride	(200)	6.292	KCl	0.549–6.00	
34	Fluorite, calcium fluoride	(111)	6.306	CaF_2	0.550-6.02	Very weak second order, strong third order.
35	Germanium	(111)*	6.532	Ge	0.570–6.23	Eliminates second order. Useful for intermediate- and low-*Z* elements where Ge $K\alpha$ emission is eliminated by pulse-height selection.
36	Potassium bromide	(200)	6.584	KBr	0.574–6.28	
37	α-Quartz, silicon dioxide	$(10\bar{1}0)$	6.687	SiO_2	0.583–6.38	P $K\alpha$ in low-*Z* matrixes, especially in calcium. Intensity for P–K *K*-lines greater than EDDT, but less than PET.

Table 4-1. *Selected data for crystals (continued).*

No.	Crystal	Miller indices	2*d* (Å)	Chemical formula	Useful wavelength region (Å)	Applications, remarks
38	Graphite	(002)	6.708	C	0.585–6.40	P, S, Cl *K*-lines, P $K\alpha$ intensity > 5X EDDT. Relatively poor resolution but high integrated reflectivity.
39	Indium antimonide	(111)	7.4806	InSb	0.652–7.23	Important for *K*-edge of Si.
40	Ammonium dihydrogen phosphate (ADP)	(200)	7.5	$NH_4H_2PO_4$	0.654–7.16	Higher intensity than EDDT.
41	Topaz	(002)	8.374	$Al_2(F,OH)_2SiO_4$	0.730–7.99	
42	α-Quartz, silicon dioxide	$(10\bar{1}0)$*	8.512	SiO_2	0.742–8.12	Same applications as EDDT and PET; higher resolution, but lower intensity.
43	Pentaerythritol (PET)	(002)	8.742	$C(CH_2OH)_4$	0.762–8.34	Al, Si, P. S, Cl $K\alpha$. Intensities ~1.5-2X EDDT, ~2.5X KHP. Good general crystal for Al–Sc $K\alpha$. Soft; deteriorates with age and exposure to x-rays.
44	Ammonium tartrate	(?)	8.80	$(CHOH)_2(COONH_4)_2$	0.767–8.4	
45	Ethylenediamine-*d*-tartrate (EDDT, EDdT, EDT)	(020)	8.808	$NH_2 \quad CH_2 - CH_2 - NH_2$ $\vert \qquad\qquad\qquad \vert$ $COOH - (CHOH)_2 - COOH$	0.768–8.40	Same applications as PET, but lower intensity, substantially lower thermal expansion coefficient. Rugged and stable.
46	Ammonium dihydrogen phosphate (ADP)	(101)*	10.640	$NH_4H_2PO_4$	0.928–10.15	Mg $K\alpha$. Same applications as PET, EDDT, but lower intensity.
47	Na β-alumina	(0004)	11.24	$NaAl_{11}O_{17}$	0.980–10.87	
48	Oxalic acid dihydrate	(001)	11.92	$(COOH)_2 \cdot 2H_2O$	1.04–11.37	
49	Sorbitol hexaacetate (SHA)	(110)	13.98	$CHOH - CO - CH_3$ $\vert$ $(COH - CO - CH_3)_4$ $\vert$ $CHOH - CO - CH_3$	1.22–13.34	Applications similar to ADP (101) and gypsum (020). High resolution; stable in vacuum. Available in small pieces only.

Table 4-1. *Selected data for crystals (continued).*

No.	Crystal	Miller indices	2*d* (Å)	Chemical formula	Useful wavelength region (Å)	Applications, remarks
50	Rock sugar, sucrose	(001)	15.12	$C_{12}H_{22}O_{11}$	1.32–14.42	
51	Gypsum, calcium sulfate dihydrate	(020)*	15.185	$CaSO_4{\cdot}2H_2O$	1.32–14.49	Na $K\alpha$. Inferior to KHP, RHP, and beryl. Poor in vacuum (efflorescent).
52	Beryl	$(10\bar{1}0)$	15.954	$3BeO{\cdot}Al_2O_3{\cdot}6SiO_2$	1.39–15.22	Difficult to obtain. Good specimens have $\lambda/\delta\lambda \sim 2500$–$3000$ at 12 Å. 2*d* may vary among specimens.
53	Bismuth titanate	(040)	16.40	$Bi_2(TiO_3)_3$	1.43–15.65	
54	Mica, muscovite	(002)*	19.84	$K_2O{\cdot}3Al_2O_3{\cdot}6SiO_2{\cdot}2H_2O$	1.73–18.93	Easy to obtain. Easily bent: good for curved-crystal spectrometers, spectrographs.
55	Silver acetate	(001)	20.0	CH_3COOAg	1.74–19.08	
56	Rock sugar, sucrose	(100)	20.12	$C_{11}H_{22}O_{11}$	1.75–19.19	
57	Na β-alumina	(0002)	22.49	$NaAl_{11}O_{17}$	1.96–21.74	
58	Thallium hydrogen phthalate (THP, TlHP, TAP, TIAP)	(100)	25.9	$TlHC_8H_4O_4$	2.26–24.7	Same applications as KHP, RHP.
59	Rubidium hydrogen phthalate (RHP, RbHP, RAP, RbAP)	(100)	26.121	$RbHC_8H_4O_4$	2.28–24.92	Diffracted intensity ~3X KHP for Na, Mg, Al $K\alpha$ and Cu $L\alpha$; ~4X KHP for F $K\alpha$; ~8X KHP for O $K\alpha$
60	Potassium hydrogen phthalate (KHP, KAP)	(100)	26.632	$KHC_8H_4O_4$	2.32–25.41	Good general crystal for all low-*Z* elements down to O.
61	Octadecyl hydrogen maleate (OHM)	(?)	63.5	$CH_3(CH_2)_{17}OOC(CH)_2COOH$	5.54–60.6	Ultralong-wavelength region down to C $K\alpha$